ANALYSIS OF BIODYNAMIC RESPONSES OF A SEATED BODY UNDER VERTICAL VIBRATION

Pranesh A.[1], Rakheja S.[1#] and DeMont R.[2]*

[1]CONCAVE Research Centre, Concordia University, Montréal (Québec), H3G 1M8, Canada
[2]Department of Exercise Science, Concordia University, Montréal (Québec), H3G 1M8, Canada
[*]anand.pranesh@gmail.com, [#]rakheja@alcor.concordia.ca

ABSTRACT

The objective assessment of occupational vibration exposure effects on the human body is largely determined from biodynamic functions obtained through measurement of the force-motion relationship at the body-seat interface. Such "driving-point" responses alone, however, may be insufficient to quantify vibratory movements of the body. The study of acceleration transmitted to the upper body may provide a deeper understanding of the human responses to vibration. In this study, an anthropometric multi-body dynamic model of the seated human body is developed to study the driving-point, vibration transmissibility and energy absorption responses to whole-body vertical vibration in the mid-sagittal plane. The model parameters are derived on the basis of the apparent mass and seat-to-head acceleration transmissibility data for 6 male subjects with comparable body mass. The inertial and geometric properties of the model are identified from the GeBOD (Generator of Body) database corresponding to mean body mass and height of the subjects employed in the measurements. The identification of visco-elastic properties of the model is explored through minimisation of three different response error functions based upon apparent mass, seat-to-head acceleration transmissibility and a combination of the two. It is shown that consideration of seat-to-head vibration transmissibility target function alone could yield reasonably good predictions of the apparent mass, seat-to-head acceleration transmissibility and the vibration power absorption in an efficient manner. The validity of the model and the parameter identification approach is demonstrated by comparing the model responses with the measured target functions. The vibration modes of the model are further derived and compared with those reported in different analytical and experimental studies. The model's capabilities are also explored to predict acceleration transmitted to the upper body segments and the power absorbed by the body.
Keywords: Biodynamics, Whole Body Vibration, Multi-Body Dynamics, Power Absorption, Vibration Transmissibility.

RÉSUMÉ

L'évaluation objective de l'effet des vibrations sur le corps humain dans le cadre du travail est en grande partie basée sur les fonctions biodynamiques. Ces fonctions sont issues de mesures de la relation force / mouvement au niveau de l'interface corps / siège ou « point d'entrée ». Toutefois, un tel point d'entrée, seul, pourrait ne pas suffire pour quantifier les mouvements vibratoires du corps. L'étude de l'accélération transmise aux différents segments du haut du corps pourrait fournir une compréhension plus approfondie des mécanismes causant les troubles de la colonne vertébrale. La présente étude élabora un modèle dynamique multi-corps du corps humain soumis aux vibrations dans une position assise. Ceci permettra d'analyser, dans le plan mi-sagittal, les réponses du système au point d'entrée, la transmissibilité vibratoire et l'absorption de l'énergie par rapport à la composante verticale des vibrations globales du corps. Les paramètres du modèle seront obtenus sur la base de la masse apparente et de la transmissibilité des accélérations siège / tête mesurées sur 6 sujets mâles avec masses corporelles comparables. Les propriétés inertielles et géométriques du modèle seront identifiées grâce à la base de données GeBOD prenant en compte les masses corporelles et tailles moyennes des sujets impliqués dans les campagnes de mesures. Les propriétés viscoélastiques du modèle seront déterminées à travers la minimisation de trois fonctions d'erreur de réponse basées sur la masse apparente, la transmissibilité des accélérations siège / tête et une combinaison des deux. Puis, il sera démontré que la prise en compte de la fonction cible de la transmissibilité siège / tête, seule, peut mener d'une manière assez efficace à des estimations raisonnablement bonnes de la masse apparente, de la transmissibilité des accélérations siège / tête et de l'absorption de la puissance vibratoire. La validité du modèle sera démontrée en comparant les réponses du modèle avec les fonctions cibles mesurées. De plus, les modes vibratoires seront obtenus et comparés avec ceux mentionnés dans différentes études analytiques et expérimentales. Les capacités du modèle seront aussi testées dans la prévision de la vibration transmise aux segments du haut du corps et de l'énergie absorbée par ceux-ci.
Mots clé: Biodynamiques, Vibrations globales du corps, Dynamiques Multi-corps, Absorption de la puissance, Transmissibilité vibratoire.

1. INTRODUCTION

Drivers of work vehicles are commonly exposed to comprehensive magnitudes of low frequency whole-body vibration (WBV), which predominate along the vertical axis in majority of the vehicles [1,2,3,4]. Epidemiological studies suggest strong relationships between WBV exposure and various health–effects [2,5,6], although a definite dose-effect relationship has not yet been identified due to the presence of a variety of confounders [7,8]. It has been widely suggested that effective biodynamic models of the human body need to be developed for predicting its responses to WBV, which could lead to a viable frequency-weighting and exposure risk-assessment methods [9,10,11]. Such models could further help in the design of effective intervention mechanisms, such as suspension seats [12,13,14,15] and anthropodynamic manikins for assessing vibration isolation performance of suspension seats [16,17]. The formulation of effective vibration bio-models, however, necessitates thorough understanding and characterisation of biodynamic responses of the body to WBV, which are known to depend on various anthropometric, posture and vibration-related factors [18,19]. These responses have been widely studied experimentally during the past three decades under broad ranges of vibration and postural conditions, which are expressed by: (i) the force-motion relations at the driving-point (DP), namely, mechanical impedance (DPMI), apparent mass (APMS) and absorbed vibratory power [e.g., 20,21,22]; and (ii) functions describing the flow of vibration "through the body", such as seat-to-head (STHT) and body segment acceleration transmissibility [e.g., 21,23,24]. These have provided considerable information on mechanical properties of the human body exposed to WBV, the influences of posture and vibration-related variables on the properties, resonance frequencies and probable modes of vibration, potential injury mechanisms and frequency-weightings for exposure assessments [18,20,25,26,27,28].

A range of lumped-parameter, multi-body and Finite Element (FE) biodynamic models of the standing and seated human body have been formulated on the basis of measured biodynamic responses, namely APMS or DPMI and/or STHT [20,28,29,30,31,32]. The properties and prediction abilities of the reported lumped-parameter models have been reviewed by Boileau et al. (1997) [33] and Liang and Chiang (2006) [34]. Multi-body and finite element models have been used for predicting vibration-induced relative deflections, and compressive and shear stresses of some of the body substructures [21,30,31,35,36], which could not be measured *in vivo*. It is desirable to develop simple yet credible biodynamic models of the seated body that may be applied for development of anthropodynamic manikins and coupled seat-occupant simulations. Owing to their simplicity, the lumped-parameter models have been traditionally applied for design and assessment of seats, and development of anthropodynamic manikins [37,38]. Such models, however, are considered valid only in the vicinity of conditions upon which their target biodynamic functions had been defined [33,34]. Moreover, these models do not relate to human anatomy and cannot yield knowledge pertinent to distribution of vibration energy or deformations of particular substructures or the effects of vibration intensity. The vibration power absorbed by the body tissue is generally a quadratic function of vibration intensity, and may thus be considered a better measure for assessing health–risks [21]. However, it has not been used in formulation or verification of biodynamic models. Simple biomechanical models based on force and moment equilibria have been applied for predicting static forces and moments at different locations of the body or spine using "link lengths" or in some cases, anthropometric measurements [39,40]. The validity of such models under WBV, however, has not been proven. More complex FE models have been employed to observe deformations and stresses in the vertebrae and inter-vertebral discs [41,42]. Such models, however, have shown limited validity in predicting biodynamic responses of the seated body to WBV and are perhaps not suited for developing anthropodynamic manikins for assessment of seats. Moreover, FE models pose extreme complexities in identification of biological parameters, particularly the dissipative properties. Alternatively, some multi-body dynamic (MBD) models have also been proposed to study human body movements under WBV. Such models generally employ lumped inertial and visco-elastic properties of selected body substructures and joints. Using the anthropometric and inertial data from a crash test dummy, Amirouche and Ider (1988) [43] constructed a three-dimensional MBD model of the sitting body with 13 rigid segments coupled through joints defined by linear stiffness and damping properties. Using visco-elastic properties from a cadaver spine, Luo and Goldsmith (1991) [44] proposed a model with lumbar and cervical spine segments to study upper body responses to shock loads. This model was further enhanced by Fritz (1998) [45] by introducing leg musculature to obtain estimates of vibration transmission, frequency-dependent muscle activity [35], and a force-based health risk weighting [46]. Yoshimura et al. (2005) [47] developed an upper body model including five lumbar segments to study relative displacements between the vertebrae. Kim et al. (2005) [48] showed that a model structure including the head, torso with a lumped visceral element, along with pelvic and thigh segments could efficiently represent multiple experimentally-measured biodynamic functions. More complex MBD models have also been attempted to study inter-vertebral forces. The spine model proposed by de Craeker (2003) [49] with muscle forces showed poor agreements with measured STHT. Verver et al. (2003) [50] integrated FE formulation of the skin tissue to an MBD spine model to derive axial and shear forces at the vertebral discs. It should be noted that the validity of the majority of the MBD models in predicting the driving-point and body segment vibration transmissibility responses, however, has not been thoroughly demonstrated. Moreover, the visco-elastic parameters of the reported models exhibit vastly different properties [30,40,43,47,48].

Considering the complex nature of the active human body and the excessive scatter of response data found in the literature [47,23,51,52] it is desirable to develop sufficiently-, but not overly-, simplified biodynamic models that incorporate representative inertial and anthropometric properties along with lumped joint properties. In the seated condition, uniaxial vertical excitation at the seat induces vertical and fore-aft body movements in the sagittal plane [23]. A sagittal plane model may thus suffice to enhance our understanding of the two-dimensional movements of the upper body under vertical vibration. Visco-elastic parameters of biodynamic models have been widely identified through minimisation of errors between the measured and model responses [10,12,20,47]. The choice of the error function, however, may have significant influences on the identified parameters and the performance of the model [53]. An appropriate error function coupled with a simplified model representing the human structure could help to identify more reliable visco-elastic parameters in an efficient manner. A model thus developed and thoroughly validated could then be used to derive certain responses that might be significant but inaccessible to conventional non-invasive techniques. This paper discusses the development of an anthropometric multi–body biodynamic model of the seated human body to study its responses to vertical WBV. A systematic methodology based upon both the driving-point force-motion relation (APMS) and the transmission of vibration (STHT) response error functions is explored for efficient visco-elastic parameter search. The vibration modes of the model are derived and compared to those published in the literature. The model is subsequently applied to predict vibration transmitted to various segments of the upper body and the distribution of vibratory power absorption due to tissue damping.

2. METHODS

2.1 Model: Structure and Joint-type Definitions

A 14-degrees-of-freedom (DOF) biodynamic model is formulated to depict the sagittal-plane vibration characteristics of a 50^{th} percentile male human seated with an erect back posture with hands-in-lap and exposed to vertical excitations from a rigid seat with no backrest interaction. Figure 1 illustrates the structure of the model consisting of seven rotational and seven translational DOF at the mid-sagittal plane. Although a two-dimensional model would be adequate for simulating the upper body motion, a three–dimensional model is formulated to account for spatial motions of the arms. The model comprises 14 inertial segments, not including the seat and vibration platform, coupled through different types of joints. As seen in Figure 1, the upper body is modelled using inertial segments representing the head, neck, upper torso (thorax), middle torso (lumbar region), abdominal viscera and the lower torso (sacro-pelvic unit). The substructures of the arms and legs are represented by two rigid bodies on both sides of the torso.

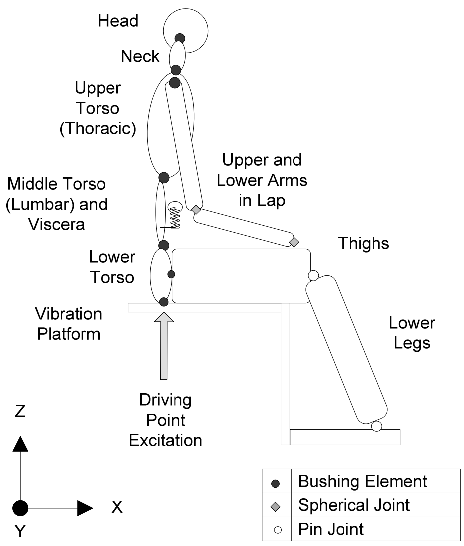

Figure 1: Sagittal plane view of the multi-body dynamic model of the body seated without a back support and exposed to vertical vibration from the seat.

Table 1: Body mass and standing height of subjects from Wang et al. (2008) [53].

Subject	Total Mass (kg)	Height (m)	Age (yrs)
1	72	1.68	39
2	73.2	1.8	26
3	74.2	1.83	25
4	77.2	1.75	25
5	77.3	1.68	38
6	79.6	1.82	26
Mean	75.6	1.76	29.8

A variety of joint-types have been employed for different segments of the model so as to balance the need for sufficient DOF and better computational efficiency. With the exception of the connections at the elbow, knee, foot and abdominal viscera, all the joints in the model are composed of "bushings" with 6-DOF, each. Each of these force–elements possesses linear stiffness and damping characteristics in both translation and rotation in all the three axes. The stiffness properties in the lateral (Y) axis and those along the roll and yaw rotations are set to extremely high values (in the order of 10^{10} N/m) in order to limit upper body movements to the sagittal plane. These constraints are imposed to reduce the size and complexity of the model, and to facilitate parameter identification for its sagittal-plane behaviour. Although muscles act as effectors and controllers in actual human movement, the properties of the muscles are lumped within the passive visco-elastic elements of the model. The visceral mass is connected to the lumbar segment by a translational visco-elasic element to permit motion along the longitudinal axis of the lumbar torso. This would ensure alignment of the viscera so as to account for any postural changes due to lumbar movements. The wrist and elbow connections are defined by spherical joints to allow for the arm's spatial motion due to lateral differences in the location of the shoulder and knee joints. The upper arms are connected to the thoracic segment through bushings so as to remove any constraint redundancy due to spherical joints at the elbow and the wrist. Further, studies have shown changes in the biodynamic responses between the "hands-in-lap" and "hands-on steering wheel" postures for the back-supported sitting conditions that may be influenced by the shoulder [53]. Pin joints are used for the knee and foot–base (ankle) connections. The upper legs (thighs) are connected to the lower torso (pelvis) through bushings to permit relative movements between the two segments, especially attributed to pelvic rotation [54].

2.2 Target Driving-Point Force-Motion and Vibration Transmission Responses

For the purpose of model parameter identification, two target datasets are identified from reported laboratory measurements of male subjects [53]. These include: (i) the force-motion relationship at the buttock-seat interface in terms of the apparent mass (APMS) of the seated body under vertical vibration; and (ii) transmission of seat vibration to the head (STHT) along the vertical axis. The measured data for a sitting posture involving hands in lap and no back support were examined to select the dataset of 6 subjects with body mass in the proximity of the 50th percentile male. The APMS, vertical and fore-aft STHT, and vibratory power absorption data were extracted for this subset of 6 males with standing mass in the range of 70 to 80 kg. The reported heights and body masses of the selected subjects are shown in Table 1 [53].

2.3 Identification of Parameters: Inertia, Anthropometry and Joint visco-elasticity

The geometric and inertial parameters of the segments considered in the model were identified from the mean body mass and height of the selected sample size using the Generator of Body (GeBOD) database on human anthropometry [55]. These included the segment masses, sagittal-plane mass moments of inertia, and the coordinates of the segments' mass centres and joints, which are summarised in Table 2. The total lumbar segment mass is partitioned in this model between the visceral mass (80%) and the lumbar skeletal structures (20%). Reported studies on various biodynamic measures under vertical vibration have shown insignificant contribution of the lower leg mass [20]. Hence, a significantly small mass of the lower leg, in the order of 1 milligram, is assumed so as to eliminate singularity in the solution process. Furthermore, the mass due to the thigh segments is adjusted to attain total model mass equal to the mean measured body mass supported by the seat, which is in the order of 78% of the total body mass [20]. This model mass value also compared quite well with the mean measured APMS magnitude at the low frequency of 0.5 Hz [53].

An error minimisation-based parameter search technique was chosen to identify the stiffness and damping characteristics of the model's joints. This seems to be a good approach due to the limited availability of reliable visco-elastic properties of biological structures. Moreover, large variability is found in properties reported in different studies [56,57]. An optimisation problem was defined as the minimisation of the weighted error between the selected measured biodynamic responses and the corresponding model outputs in the frequency domain. The target responses in terms of APMS and vertical STHT magnitude and phase were considered, as described above.

Table 2: Anthropometry and inertial properties of the human body model.

Segment	Mass (kg)	Mass Moment of Inertia (kg.m^2)	Coordinates (m)		
			X	Y	Z
Head	5.038	0.031	0.024	0.000	0.644
Neck	1.293	0.003	0.025	0.000	0.507
Upper Torso	17.343	0.136	0.012	0.000	0.275
Middle Torso	1.996	0.033	0.003	0.000	0.074
Viscera	7.986	-	0.003	0.000	0.094
Lower Torso	8.570	0.038	0.008	0.000	-0.048
Thigh (each)	5.13	0.106	0.207	± 0.060	-0.081
Lower Leg (each)	10^{-6}	10^{-6}	0.455	± 0.080	-0.256
Upper Arm (each)	1.991	0.014	0.037	± 0.193	0.253
Lower arm (each)	1.994	0.010	0.213	± 0.137	0.044
Joint Location					
Upper neck			0.008	0.000	0.591
Lower neck			-0.001	0.000	0.473
Shoulder			0.000	-0.193	0.377
Thoracic – Lumbar			-0.014	0.000	0.163
Lumbar – Pelvic			0.000	0.000	0.000
Pelvic – Seat			0.000	0.000	-0.167
Hip (Y is ±)			0.016	0.080	-0.097
Knee (Y is ±)			0.405	0.080	-0.081
Ankle (Y is ±)			0.505	0.080	-0.488
Elbow (Y is ±)			0.076	0.193	0.112
Wrist (Y is ±)			0.350	0.080	-0.023

In order to account for the strong frequency dependence of the biodynamic responses, the error function for each response parameter was defined as the weighted sum of errors in four discrete frequency bands, such that:

$$E_k(\mathrm{X}) = a_1 \sum_{f_i=0.5}^{2} e^2(f_i) + a_2 \sum_{f_i=2.025}^{7} e^2(f_i) + a_3 \sum_{f_i=7.025}^{10} e^2(f_i) + a_4 \sum_{f_i=10.025}^{15} e^2(f_i) \qquad (1)$$

Where, $E_k(\boldsymbol{X})$ is the frequency–weighted error function of the parameter vector $\boldsymbol{X}$ in the response variable k (e.g. APMS) either in its magnitude (M) or phase (ϕ). Constants a_1, a_2, a_3 and a_4 are the weights for the four frequency bands (0.5-2, 2.025-7, 7.025-10, and 10.025-15 Hz), and e is the error between a model response parameter and the target value corresponding to excitation frequency f_i. The above function may be conveniently used to compute error in the response magnitude or phase or both, with different weighting of errors in different frequency bands. A relatively larger weighting around the primary resonance band (2-7 Hz), i.e. a_2, would probably be desirable for faster convergence. Individually, the error functions in APMS and STHT may be defined as:

$$E_{APMS}(\mathrm{X}) = \alpha_A E_{AM}(\mathrm{X}) + \beta_A E_{A\phi}(\mathrm{X}) \quad (2)$$

$$E_{STHT}(\mathrm{X}) = \alpha_S E_{SM}(\mathrm{X}) + \beta_S E_{S\phi}(\mathrm{X}) \quad (3)$$

Where, $E_{APMS}(X)$ and $E_{STHT}(X)$ are the composite errors in APMS and STHT magnitude (E_{AM} and E_{SM}) and phase ($E_{A\phi}$ and $E_{S\phi}$), respectively. Furthermore, different weights, α and β, are imposed on the magnitude and phase errors of the APMS and STHT, respectively, to ensure their comparable contributions to the total error function, given by:

$$E(\mathrm{X}) = \lambda_A E_{APMS}(\mathrm{X}) + \lambda_S E_{STHT}(\mathrm{X}) \quad (4)$$

The above minimisation problem may be solved to identify model parameters on the basis of APMS error alone (λ_A=1 and λ_S=0) or the STHT error alone (λ_A=0 and λ_S=1) or both errors (λ_A=λ_S=1). The vast majority of the lumped parameter models, with only a few exceptions, have been derived on the basis of APMS alone [20, 34]. It has been shown that the APMS response describes the dynamic body-seat interactions at the driving-point alone, while the STHT being a through–the–body function emphasises the vibration modes of the upper body [53]. The STHT may thus be a better measure for parameter identification, since it indirectly accounts for the vibration modes associated with different upper body segments. It may thus be hypothesised that minimisation of $E_{STHT}(X)$ alone could yield identification of more reliable model parameters than the $E_{APMS}(X)$ alone. The minimisation problems for different combinations of λ_A and λ_S were solved in the frequency-domain subject to a number of limit and inequality constraints on the model parameters. Limit constraints for the stiffness values of the bushings in the upper torso structure were defined on the basis of reported ranges of cadaver values [56,57], while the damping parameters were constrained to positive values. The initial parameter vector was mostly based on the model parameters reported by Amirouche and Ider (1988) [43]. A gradient–based search algorithm (Sequential Quadratic Polynomial) was used to solve the minimisation problem, defined in Eqs. (2) to (4). Solutions were attained for a large number of different starting parameter vectors and weighting values. The convergence to a solution was assumed if two or more successive iterations of the search resulted in deviations in error magnitude less than 0.01. Furthermore, a check for local optima was performed by perturbing each variable in the final parameter vector within 10% of the identified value. Parameter identification was conducted using three different error functions: (i) based upon APMS error alone, as defined in Eq. (2), referred to as 'Model-A'; (ii), STHT error alone, as defined in Eq. (3), referred to as 'Model-S'; and combined error function, as defined in Eq. (4), referred to as 'Model-AS.'

The differential equations of motion for the model were solved using the GStiff integrator in the multibody dynamic code, MSC ADAMS [58]. Initial static tests with gravity showed a stable settling of the model on the rigid seat. The analyses were performed under sinusoidal displacement excitation at the seat platform swept in the 0.5 to 15 Hz range, while the displacement amplitude corresponding to each excitation frequency was selected to achieve a flat 1 m/s^2 RMS acceleration spectrum to simulate the conditions of the experiment. The equations of motion were linearised and solved in the frequency domain with the assumption of small joint motions.

2.4 Model Outputs

A comparison between the measured biodynamic functions and the simulation responses was first made in order to assess the models' performance. The model with the best performance was considered for further analyses. The natural frequencies, modal damping ratios and vibration modes of the chosen model were computed through solution of the eigen-value problem. Also, frequency responses in terms of the acceleration transmissibility from the seat to various segments of the model were derived for the chosen model. Furthermore, the ability of the model to predict absorbed power was explored by considering energy dissipated by the viscous elements, such that:

$$P_{abs}\left(f_i\right)=\sum_j c_j \bar{v}_j^2+\sum_j c_{rj}\bar{v}_{rj}^2 \tag{5}$$

Where P_{abs} is the absorbed power response value at a discrete frequency f_i, and c_j and c_{rj} are viscous damping coefficients of joint j in translation and rotation, respectively. $\bar{v}_j$ and $\bar{v}_{rj}$ are the RMS translational and rotational relative velocities, respectively, across joint j. In a constant bandwidth analysis, used in this simulation, the spectral density of power absorption can be obtained by normalising P_{abs} by the fixed frequency resolution ($f_{i+1}-f_i$). This permits for direct comparison with the reported measured data that have been presented in terms of the spectral density. It should be noted that the absorbed power response characteristics of the seated body under WBV have been traditionally derived experimentally from driving-point measures, such as mechanical impedance or apparent mass [21]. However, the absorbed power analysis of this model incorporates relative movement of different body segments occurring at the joints, which are not directly measurable.

3. RESULTS

3.1 Biodynamic Responses

Although all the three minimisation approaches resulted in reasonably good convergence to the respective target datasets, Model–A based on APMS error resulted in notable deviations in the phase response at higher frequencies (above 8 Hz). The Models–S and –AS resulted in similar convergence to the solutions, while the solution of Model–AS was far more computationally demanding due to consideration of both APMS and STHT errors. The discussions of the results presented further are thus limited to Model–S only. Figures 2 illustrates biodynamic responses from the two approaches: Model–A and Model–S. The results show that Model-A yields relatively poor agreement in the STHT response, particularly in its phase, as shown in Figure 2(a). Model–S based on vertical STHT error minimisation provided excellent agreement in STHT response with some error in the APMS response at frequencies above 8 Hz, as seen in Figure 2(b). Both the approaches reveal primary resonance near 4.75 Hz depicted by peaks in both APMS and STHT magnitude responses. While Model–A shows reasonably good agreements in APMS and STHT magnitudes at frequencies below 7 Hz, the STHT response peak near 3 Hz is not evident in the model response, which has been associated with pitch rotation of the upper body [23]. Furthermore, Model–A responses show slight secondary peak in the STHT response near 10 Hz, while this peak in the target response occurs at a lower frequency (8-9 Hz). Considerable errors are also evident in the STHT phase responses of this model, particularly at frequencies above 7 Hz.

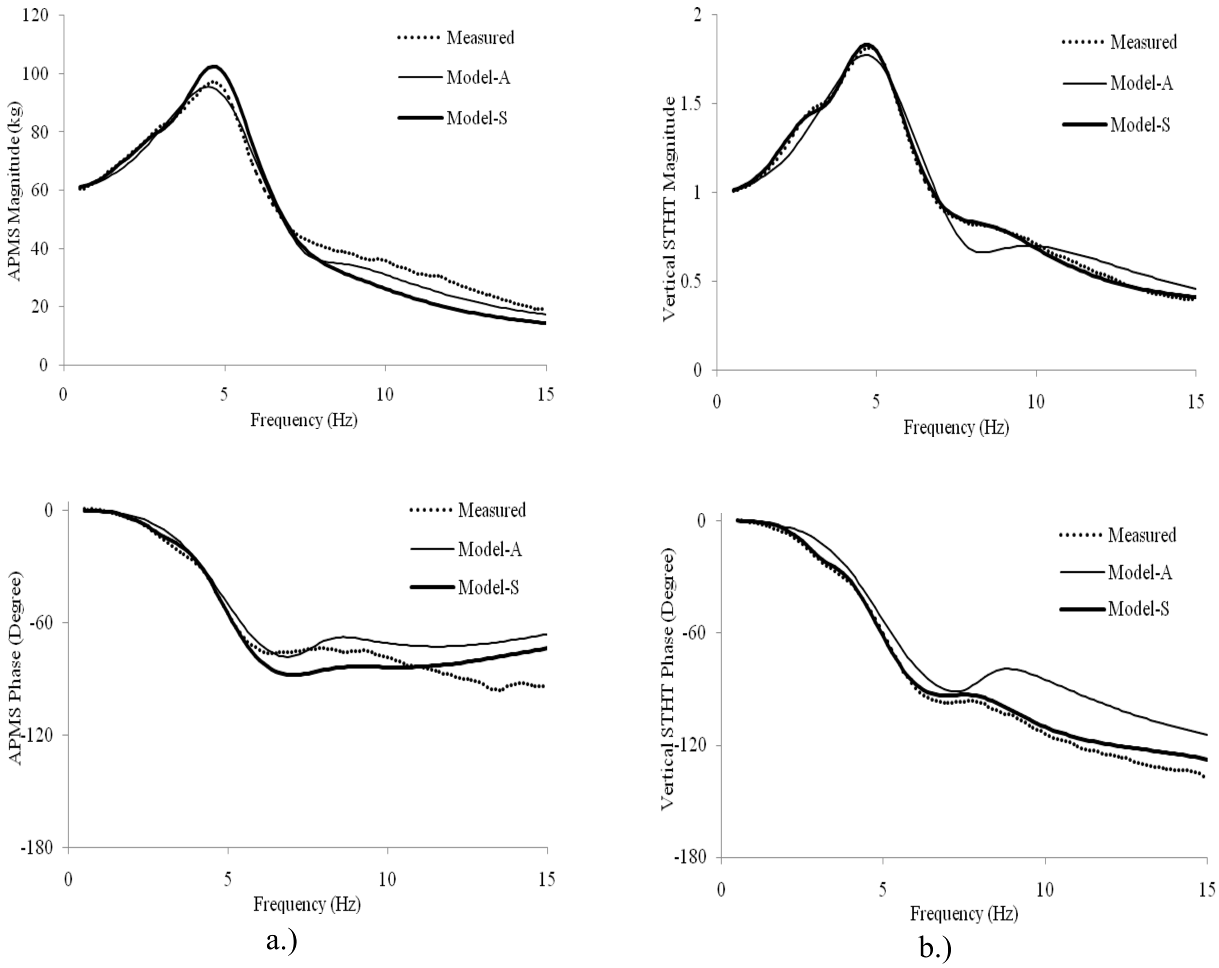

Figure 2: Comparison of Models–A and Model–S responses with mean measured functions [53] a.) Apparent mass (APMS); b.) Vertical seat-to-head acceleration transmissibility (STHT).

Model–S yields considerably better agreements in the STHT magnitude and phase responses, as evidenced in Figure 2(b). The STHT response of the model shows peaks near 3, 4.75 and 8 Hz, which are identical to those observed in the target response. The APMS magnitude response also reveals a slight peak near 3 Hz that was observed in the target data. From the results, it may be concluded that the model based on minimisation of error in the STHT responses could also yield reasonably good prediction of the APMS response. The visco-elastic parameter values identified from the two approaches are presented in Table 3.

Both the models were subsequently solved to compute the horizontal (fore-aft) STHT magnitude, although it was not included in the minimisation function. Figure 3 shows this response from the two models along with the mean measured data from the selected 6 subjects. While both the models show considerable errors in response magnitude, Model-S yields relatively smaller deviations compared to Model-A. The horizontal STHT magnitude peak of the model occurring near 3 Hz may be attributed to upper body pitch coupled with fore-aft translation of the pelvis, while the measured responses exhibit peak near 4 Hz. Moreover, the peak fore-aft STHT magnitude of 1.19 was observed to be considerably larger than the value around 0.75 that was reported by Paddan and Griffin (1998) [24]. More reliable measurements are thus desirable, which may yield improved parameter identification when integrated in the error function in the minimisation problem. In summary, the results suggest that parameters identified from Model–A could be considered sufficient to represent the driving-point dynamic behaviour of the seated body, while Model–S may yield better description of the upper body vibratory motion.

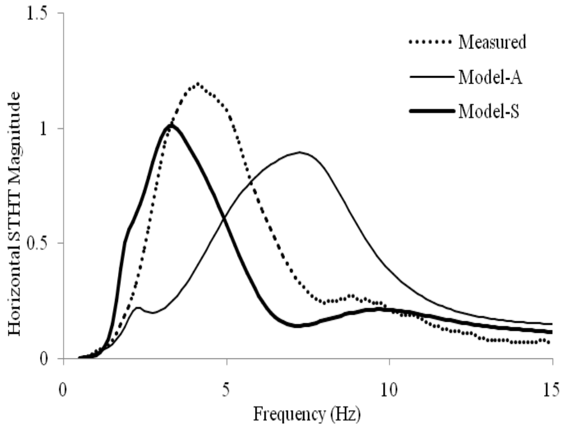

Figure 3: Comparison of horizontal STHT magnitude of Model–A and Model–S with the mean measured curve.

Table 3: Visco-elastic joint properties identified through optimisation for Model-A and Model-S.

Stiffness* (N/m , N-m/rad)				Damping* (N-s/m , N-m-s/rad)			
	Initial	Model–A	Model–S		Initial	Model–A	Model–S
K head	120000	68264.87	68541.95	C head	1500	502.52	502.52
K_r head	1200	418.37	120.00	C_r head	20	10.45	0.82
K neck	120000	1911196.3	56017.90	C neck	1500	1889.16	1888.09
K_r neck	1200	11.10	30.00	C_r neck	20	0.70	0.70
K up torso	105000	396517.77	628760.65	C up torso	1600	2257.84	2258.71
K_r up torso	2200	777.21	533.00	C_r up torso	40	8.14	35.01
K shoulder	100000	673220.02	23156.39	C shoulder	1000	149.74	128.43
K_r shoulder	100	295.32	445.92	Cr shoulder	1	42.28	10.00
K lumbar	105000	169511.9	431294.15	C lumbar	1800	2032.85	2011.06
K_r lumbar	2200	1287.98	1313.00	C_r lumbar	40	27.96	35.52
K viscera	5000	20641.27	16908.40	C viscera	50	316.12	159.38
K buttock	20000	53787.53	38596.52	C buttock	1100	1797.24	1226.04
K_x buttock	10000	108337.68	11385.51	C_x buttock	1	485.98	95.64
K_r buttock	1300	18920.91	18920.91	C_r buttock	30	5.62	5.62
K_x thigh	10000	$159.42\text{x}10^5$	$159.42\text{x}10^5$	C_x thigh	1000	47.36	54.59
K_r thigh	5000	1617.68	1617.68	C_r thigh	1	15.36	15.36

* Variables: K, C – Translational Vertical; K_X, C_X – Translational Horizontal; K_r, C_r – Pitch

3.2 Modal Properties

Eigen analysis of Model–S revealed the presence of 7 modes at frequencies below 20 Hz. The natural frequencies and modal damping ratios of these modes are summarised in Table 4. The first two modes occurring near 1.8 and 3.14 Hz correspond to shear (X-axis translation) of the buttock tissue coupled with out-of-phase and in-phase thoracic pitch, respectively. A vertical whole body mode is evident near the natural frequency of 5.07 Hz, which was primarily associated with deformation of the buttock tissue in the vertical and shear directions coupled with lumbar vertical stretch and slight visceral movement. The fourth at 8.12 Hz was a visceral mode coupled with head-neck vertical movement. A few other modes were also found at higher frequencies. Head pitch about the neck joint was observed at 9.6 Hz, and two vertical shoulder modes were observed at 13.46 and 14.94 Hz.

3.3 Acceleration Transmitted to Body Segments

Model–S was subsequently solved to study vibration transmissibility to its various segments. Figure 4 shows the vertical acceleration transmissibility to the segments representing the head, upper torso (at T1-Thoracic vertebral unit 1), mid torso (L3-Lumbar 3) and the pelvis. The results clearly show systematic progression of vertical vibration transmission from the lower to the higher segments in the frequency range considered. This progression is particularly evident between 3-11 Hz. The head response reveals a slight peak near 3 Hz, which is not evident in the T1, L3 and the pelvic responses. Near primary resonance, the difference in vertical acceleration transmissibility seems to be larger between the lumbar and the pelvic segments than that between the lumbar and the upper torso. This is suggestive of significant relative vertical movement in the lower region of the torso, indicative of higher vibration loads and/ or compression-extension in the lumbar torso.

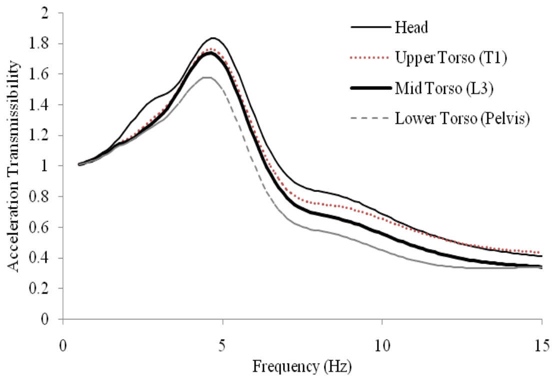

Figure 4: Vertical acceleration transmissibility magnitude between the seat and upper body segments of Model-S.

Table 4: Modal properties of Model-S.

Mode	Undamped Natural Frequency (Hz)	Damping Ratio
1	1.80	0.16
2	3.14	0.27
3#	**5.07**	**0.30**
4	8.12	0.29
5	9.60	0.24
6	13.46	0.29
7	14.94	0.35

#Dominant mode

3.4 Vibration Power Absorption

The absorbed power response of the model derived on the basis of STHT target data (Model–S) are compared with the mean measured absorbed power reported by Wang et al. (2006) [24] extracted for the same six subjects used in this study, as shown in Figure 5. The model shows reasonably good agreement with the measured data in the entire frequency range, except for slight deviation in the peak magnitude. These findings suggest that the model derived on the basis of STHT target data is also able to predict the total absorbed power response reasonably well.

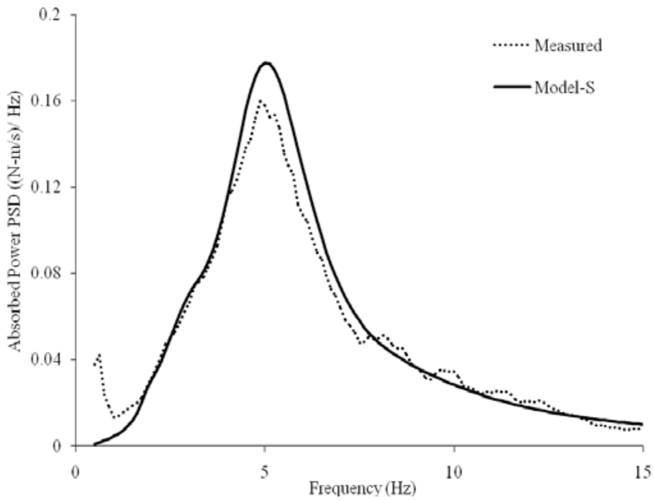

Figure 5: Spectral density of the Total Absorbed Power response of Model-S with the mean measured curve from 6 subjects evaluated at the driving point [22].

4. DISCUSSIONS

Apparent mass is the most widely reported seated body response to WBV in the literature. This function can be obtained with minimal non-invasive instrumentation at the driving-point, namely, the seat-buttock interface. Being measured at the input point only, the apparent mass response may not be capable of completely describing the two dimensional body movements at the mid-sagittal plane. The STHT measure, on the other hand, may be considered to include the vibration responses of different body segments and transmission of vibration through the spine, albeit indirectly. It has been reported that the STHT function could better relate to the effects of back support and posture than the APMS response [53]. STHT, however, exhibits far greater variability than APMS, attributed to the former's higher sensitivity to variations in independent parameters, namely the dynamic properties of the head acceleration measurement system, involuntary head movements during an experiment and experimental conditions [24]. As seen from Figures 2 and 3, the visco-elastic parameters of the model identified on the basis of APMS target data alone could match the driving-point measure reasonably well, while those based upon STHT targets could lead to satisfactory agreements in both the APMS and STHT responses. Further, the minimisation function based upon the summation of APMS and STHT errors also resulted in responses similar to those obtained with STHT target data alone, but was far more computationally cumbersome. Hence, it can be inferred that employing an STHT target function alone would be adequate for identifying model parameters for describing both the driving-point and head vertical response measures in an efficient manner. The validity of the approach and thus the model, however, requires additional target responses involving vibration measurements at different body segments. Only a limited number of studies have reported such segmental responses [47,23,51,52,54] and only little agreement could be observed in the reported data. In this study, the model's validity has been further explored in terms of its ability to predict the total vibration absorbed power. The vibration energy dissipated by the viscous elements compares quite well with the total power measured at the driving-point (Figure 5).

The model established on the basis of the STHT target function revealed seven vibration modes below 20 Hz. Pankoke et al. (1998) [41] reported a spine bending mode near 2.75 Hz, while Kim et al. (2005) [48] found a "spine, visceral and head fore-aft" mode at 2.71 Hz. The modal experiments performed by Kitazaki and Griffin (1998) [54] revealed two modes with a coupled head-neck and pelvis fore-aft motion opposed-to and in-phase with each other at 2.2 and 3.4 Hz, respectively. The model in the present study showed two modes of thoracic spine bending about the upper lumbar joint coupled with buttock shear in opposed-phase and in-phase at 1.8 and 3.14 Hz, respectively. The secondary peak in the STHT responses at frequencies below 4 Hz (Figure 2b) may be associated with these two modes. Furthermore, the primary peak in head fore-aft vibration transmissibility (Figure 3) may be attributed to the second mode near 3.14 Hz. Although this is not clearly seen in the mean APMS response, the shear of the buttock tissue associated with the above modes may contribute to the low frequency peak observed in the individual data for some of the subjects [53]. The primary vertical vibration mode, widely reported to occur in the 4 to 6 Hz range, has been generally associated with whole body vertical vibration due to buttock compression and shear. Experiments by Kitazaki and Griffin (1998) [54] also showed visceral movement at the primary resonance mode around 5 Hz. These authors also showed an additional mode with lumbar and lower thoracic spine bending and head vertical motion at 5.6 Hz [54], while Model–S in this study shows one coupled mode near 5.1 Hz. A visceral mode has been reported in the 8 to 14 Hz range in the published literature [41,48,54]; Model–S revealed this mode near 8.1 Hz. The head pitch mode of the model occurs near 9.6 Hz, which is considerably lower than the 16.67 Hz reported by Amirouche and Ider (1988) [43]. The shoulder mode has been reported to occur at 11.4 Hz in only one study [41], which was observed near 14 Hz in the model. With the wide variability in the reported vibration modes, which are mostly attributed to complex movements of the human body, the effects of torso-muscular activity and the presence of highly non-linear damping [54], it may be difficult to understand the modal behaviour of the human body through simple linearised models. Although the model proposed in this study shows satisfactory agreement with significant modes reported in the literature, additional measurement and modelling efforts are vital for improving its reliability.

The model's segmental vibration responses (Figure 4) reveal inconclusive results when compared with experiments performed by Matsumoto and Griffin (2001) [23]. A peak in the vertical response magnitude at all levels of the upper body around the APMS resonant frequency measured by Matsumoto and Griffin (2001) [23] is also evidenced in the model results. However, there are considerable differences in the peak magnitude values. Also, the same authors [23] show peaks in the horizontal STHT magnitude at frequencies above the resonance; the model in this study shows somewhat different results. It should be noted, however, that the subjects in the compared study [23] sat with legs hanging, which may account for the differences. Similarly, wide variability in the reported data on the vibration responses measured at different levels of the upper body could be seen, whether measured *in vivo* [51,52] or by non-invasive methods [19,21,23,47,54]. A variety of factors including the type and location of sensors, subject anthropometry, posture, seating conditions and input excitation levels could influence these response characteristics. Further efforts in establishing segmental responses to WBV with careful attention to influence parameters would thus be vital for verification and enhancement of biodynamic models. The resulting models could then be applied for predicting distribution of vibration energy in the joints under different independent conditions, which may give an insight into the potential injury risks in different types of WBV environments.

5. CONCLUSIONS

An anthropometric multi-body biodynamic model of the seated human body exposed to vertical vibration at the seat was developed to study the vibration behaviour of different segments of the human body. Visco-elastic parameters of the model were identified through minimisation of error functions in apparent mass, seat-to-head vibration transmissibility and a combination of the two. It was concluded that vertical head acceleration transmissibility is a better target dataset for parameter search than the apparent mass, since it represents indirectly the vibration transmission through different segments of the upper body. Additionally, the model thus derived was also able to provide a reasonably good prediction of total vibration power absorption by the body. Modal properties of the model revealed seven modes below 20 Hz some of which were comparable with those reported in the published literature. The model was further applied to evaluate the nature of vibration transmission its segments. The results of this study suggest that the widely used apparent mass and seat-to-head vibration transmission functions need to be augmented with vibration measures at different body segments in order to develop more reliable models capable of predicting the movements of the seated human body and distribution of vibration power absorption. Further experimental works are thus necessary to quantify the segmental responses of the human body in a reliable manner.

6. REFERENCES

1. Mansfield N.J., 2003 Effect of increasing measurement duration on accuracy of whole-body vibration field measurements, Proc. of the 38th UK Group Meeting on Human Response to Vibration, Gosport, UK, 17-19 September.
2. Bovenzi M., Pinto I. and Stacchini N., 2002, Low back pain in port machinery operators, Journal of Sound and Vibration, 253(1): 3-20.
3. Bovenzi M., Rui F., Negro C., D'Agostin F., Angotzi G., Bianchi S., Bramanti L., Festa G.L., Gatti S., Pinto I., Rondina L. and Stacchini N., 2006, An epidemiological study of low back pain in professional drivers, Journal of Sound and Vibration, 298: 514-539.
4. Okunribido O.O., Magnusson M., Pope M., 2006, Low back pain in drivers: The relative role of whole-body vibration and manual materials handling, Journal of Sound and Vibration, 298: 540-555.
5. Bongers P.M., Boshuizen H.C., Hulshof C.T.J., Koemeester A.P., 1988, Back disorders in crane operators exposed to whole-body vibration, Int. Arch. Occ. Env. Health, 60: 129-137.
6. Bovenzi M. and Zadani A., 1992, Self-reported back symptoms in urban bus drivers exposed to

whole body vibration, Spine, 17: 1048-59.

7. Seidel H. and Heide R., 1986, Long term effects of whole-body vibration: A critical survey of literature, Int. Arch. Occ. Env. Health, 58: 1-26.
8. Lings S., Leboeuf-Yde C., 2000, Whole-body vibration and low back pain: asystematic critical review of the epidemiological literature 1992-1999, Int. Arch. Occ. Env. Health, 73: 290-297.
9. Seidel H., 2005, On the relationship between whole-body vibration exposure and spinal health risk, Industrial Health, 43: 361-377.
10. Griffin M.J., 2001, The validation of biodynamic models, Clinical Biomechanics, 16(Suppl. 1): S81-S92.
11. Hinz B., Menzel G., Blüthner R. and Seidel H., 2001, Transfer functions as a basis for the verification of models – variability and restraints, Clinical Biomechanics, 16(Suppl. 1): S93-S100.
12. Tchernychouk V., Rakheja S., Stiharu I. and Boileau P-É., 2000, Study of occupant-seat models for vibration comfort analysis of automotive seats, Transactions of SAE, J. of Passenger Vehicles- Mechanical Systems, 109(6): 2308-2313.
13. Wei L. and Griffin M.J., 1998, The prediction of seat transmissibility from measures of seat impedance, Journal of Sound and Vibration, 214(1): 121-137.
14. Pang J., Qatu M., Rao D., Sheng G., 2005, Nonlinear seat cushion and human body model, International J. of Vehicle Noise and Vibration, 1(3/4): 194-206.
15. Stein G.J. and Múča P., 2003, Theoretical investigation of a linear planar model of a passenger car with seated people, Proc. of Instn. Mech. Engrs., J.of Automobile Engineering, 217: 257-268.
16. Toward M.G.R., 2001, Effect of backrest interaction on seat cushion transmissibility, Proc. of the 36th UK Group Meeting on Human Response to Vibration, Farnborough, UK, 12-14 September: 106-115.
17. Cullmann A. and Wölfel H.P., 2001, Design of an active vibration dummy of sitting man, Clinical Biomechanics, 16(Suppl. 1): S64-S72.
18. Wang W., Rakheja S. and Boileau P-É., 2004, Effects of sitting postures on biodynamic response of seated occupants under vertical vibration, International Journal of Industrial Ergonomics, 34(4): 289-306.
19. Mansfield N.J. and Griffin M.J., 2002, Effects of posture and vibration magnitude on apparent mass and pelvis rotation during exposure to whole-body vertical vibration, Journal of Sound and Vibration, 253(1): 93-107.
20. Fairley T.E. and Griffin M.J., 1989, The apparent mass of the seated human body: vertical vibration, J. of Biomechanics, 22: 81-94.
21. VIN – Vibration Injury Network, 2001, Review of methods for evaluating human exposure to whole-body vibration, Appendix W4A to Final Report.
22. Wang W., Rakheja S. and Boileau P-É., 2006, The role of seat geometry and posture on the mechanical energy absorption characteristics of seated occupants under vertical vibration, Intl. J. Indus. Ergo., 36: 171-184.
23. Matsumoto Y., Griffin M.J., 2001, Movement of the upper body of seated subjects to vertical whole body vibration at the principal resonance frequency, J. Sound Vib., 215 (4): 743-762.
24. Paddan G.S., Griffin M.J., 1998, A review of the transmission of translational seat vibration to the head, J. Sound Vib., 215 (4): 863-882.

25. Hinz B., Seidel H., Menzel G. and Blüthner R., 2002, Effects related to random whole-body vibration and posture on a suspended seat with and without backrest, Journal of Sound and Vibration, 253(1): 265-282.
26. Mansfield N.J. and Maeda S., 2005, Comparison of the apparent mass of the seated human measured using random and sinusoidal vibration, Industrial Health, 43: 233-240.
27. Nawayseh N. and Griffin M.J., 2005, Non-linear dual-axis biodynamic response to for-and-aft whole-body vibration, Journal of Sound and Vibration, 282: 831-862.
28. Rakheja S., Stiharu I., Zhang H. and Boileau P-É., 2006, Seated occupant interactions with seat backrest and pan, and biodynamic responses under vertical vibration, J. of Sound and Vib., 298: 651-671.
29. Mertens H., 1978, Nonlinear behaviour of sitting humans under increasing gravity, Aviation Space and Environmental Medicine, 49: 287-298.
30. Fritz M., 2005, Dynamic properties of the biomechanical model of the human body – influence of posture and direction of vibration stress, J. of Low Freq. Noise, Vib. and Active Control, 24(4): 233-249.
31. Pankoke S., Hofmann J. and Woelfel H.P., 2001, Determination of vibration-related spinal loads by numerical simulation, Clinical Biomechanics, 16(Suppl. 1): S45-S56.
32. Boileau P-É. and Rakheja S., 1998, Whole-body vertical biodynamic response characteristics of the seated vehicle driver: Measurement and model development, International Journal of Industrial Ergonomics, 22(6): 449-472.
33. Boileau P-É., Rakheja S., Yang X. and Stiharu I., 1997, Comparison of biodynamic response characteristics of various human body models as applied to seated vehicle drivers, Noise and Vibration Worldwide, 28 (9): 7-15.
34. Liang C. and Chiang C., 2006, A study of biodynamic models of seated human subjects exposed to vertical vibration, Int. J. of Ind. Ergonomics, 36: 869-890.
35. Fritz M., 2000, Simulating the response of a standing operator to vibration stress by means of a biomechanical model, Journal of Biomechanics, 33: 795-802.
36. Liu X.X., Shi J. and Li G.H., 1998, Biodynamic response and injury estimation of ship personnel to ship shock motion induced by underwater explosion, Proc. of 69th Shock and Vibration Symp., St. Paul., Vol. 18: 1-18.
37. Lewis C.H., 2005, Variability in measurements of seat transmissibility with an active anthropodynamic dummy and with human subjects, 40th UK Group Meeting on Human Response to Vibration.
38. Mansfield N.J., Griffin M.J., 1996, Vehicle seat dynamics measured with an anthropodynamic dummy and human subjects, Proceeding of the Inter-Noise'96, Vol. 4: 1725-1730.
39. Keller T., Colloca C.J., Beliveau J-G., 2002, Force-deformation response of the lumbar spine: A sagittal plane model of posteroanterior manipulation and mobilisation, Cli. Biomechanics, 17: 185-196.
40. Kim S.K., White S.W., Bajaj A.K., Davies P., 2003, Simplified models for the vibration of mannequins in car seats, J. Sound Vib., 264 (1): 49-90.
41. Pankoke S., Buck B., Woelfel H. P., 1998, Dynamic FE model of sitting man adjustable to body height, body mass and posture used for calculating internal forces in the lumbar vertebral disks, J. Sound Vib., 215 (4): 827-839.
42. Seidel H., Bluthner R., Hinz B., 2001, Application of finite-element models to predict forces

acting on the lumbar spine during whole-body vibration, Cli. Biomech., 16 Suppl. (1): S57-63.
43. Amirouche F.M.L. and Ider S.K., 1988, Simulation and analysis of a biodynamic human model subjected to low accelerations - a correlation study, J. Sound Vib., 123 (2): 281-292.
44. Luo Z., Goldsmith W., 1991, Reaction of a human head/ neck/ torso system to shock, J. Biomechanics, 24 (7): 499-510.
45. Fritz M., 1998, Three-dimensional biomechanical model for simulating the response of the human body to vibration stress, IEEE Med. Bio. Engg. and Computation, 36: 686-692.
46. Fritz M., Fischer S., Brode P., 2005, Vibration-induced low back disorders - comparison of the vibration evaluation according to ISO 2631 with force-related evaluation, Appl. Ergo., 36: 481-488.
47. Yoshimura T., Nakai K., Tamaoki G., 2005, Multi-body dynamics modeling of seated human body under exposure to whole-body vibration, Indus. Health, 43: 441-447.
48. Kim T., Kim Y., Yoon Y., 2005, Development of biomechanical model of the human body in a sitting posture with vibration transmissibility in the vertical direction, Intl. J. Indus. Ergo., 35: 817-829.
49. De Craecker W., 2003, Whole-body vibration comfort analysis based upon spine modelling, 38th UK Conf. HRV, Southampton, UK.
50. Verver M.M., van Hoof J., Oomens C.W.J., van de Wouw N., Wismans J.S.H.M., 2003, Estimation of spinal loading in vertical vibrations by numerical simulation, Cli. Biomech., 18: 800-811.
51. Panjabi M.M., Anderson G.B.J., Jorneus L., Hult E., Mattson L., 1986, *In vivo* measurement of spinal column vibrations, J. Bone Joint Surg., 68-A (5): 695-702.
52. Pope M.H., Kaigle A.M., Magnusson M.L., 1991, Intervertebral motion during vibration, Proc. Inst. Mech. Engg., 205: 39-44.
53. Wang W., Rakheja S. and Boileau P-É., 2008, Relationship between measured apparent mass and seat-to-head transmissibility responses of seated occupants exposed to vertical vibration, Journal of Sound and Vibration, 314(5): 907-922.
54. Kitazaki S., Griffin M.J., 1998, Resonance behaviour of the seated human body and effects of posture, J. Biomechanics, 31 (2): 143-149.
55. Cheng H., Obergefell L., Rizer A., 1994, Generator of body (GEBOD) Manual, Report No. AL/CF-TR-1994-0051, Amstrong Laboratory, Wright-Patterson Air Force Base, Ohio.
56. Gardner-Morse M.G., Stokes I.A.F., 2004, Structural behaviour of human lumbar spine motion segments, J. Biomechanics, 37: 205-212.
57. Panjabi M.M., Brand R., White III A.A., 1976, Three-dimensional flexibility and stiffness properties of the human thoracic spine, J. Biomechanics, 9: 185-192.
58. User's Manual MSC.ADAMS, MSC.Software Corp., Santa Ana, California, USA.

7. AUTHOR BIOGRAPHIES

Anand M-Pranesh is a Doctoral Candidate in Mechanical Engineering working at the Concordia Centre for Advanced Vehicle Engineering (CONCAVE), Concordia University, Montréal, Canada. His research work involves the study of vibration in the human musculoskeletal spine. He is keen on specialising in the area of vibrations – measurement systems and modelling.

Subhash Rakheja, PhD, Fellow of the ASME, is a Professor of Mechanical Engineering and Vehicular Ergodynamics Research Chair at the Concordia Centre for Advanced Vehicle Engineering (CONCAVE), Concordia University, Montréal, Canada. He is also a Fellow of the Canadian Society of Mechanical Engineers. His research interests lie in dynamics of heavy vehicles, particularly the partly-filled liquid cargo vehicles, vehicle suspension, ride dynamics of road and off-road vehicles, human responses to whole-body and localised vibration, and biodynamics.

Richard DeMont, Ph.D., is Associate Professor in the Department of Exercise Science at Concordia University, Montréal, Canada. A certified Athletic Therapist and Chair at the Program Accreditation Committee of the Canadian Athletic Therapists Association (CATA), he is also Director of the Athletic Research Laboratory at Concordia. He works in close association with CONCAVE studying the musculoskeletal loading of seated occupational drivers exposed to whole body vibration; vibration control and optimal postural support condition.